Commensurability and stability in nonperiodic systems

Y. Fasano*†, M. De Seta‡, M. Menghini*§, H. Pastoriza*, and F. de la Cruz*

*Instituto Balseiro and Centro Atómico Bariloche, Comisión Nacional de Energía Atómica, 8400 Bariloche, Argentina, and ‡Dipartimento di Fisica, Universitá di Roma Tre, 00146 Rome, Italy

This contribution is part of the special series of Inaugural Articles by members of the National Academy of Sciences elected on April 30, 2002.

Contributed by F. de la Cruz, December 13, 2004

We have investigated the response of 3D $Bi_2Sr_2CaCu_2O_8$ vortex structures to a weak perturbation induced by 2D Fe pinning structures acting on one extremity of vortex lines. The pinning patterns were nano-engineered at the sample surface by means of either a Bitter decoration of the vortex lattice or electron-beam lithography. The commensurability conditions between 2D rigid pinning potentials and 3D elastic structures with short-range positional and long-range orientational correlation have been experimentally determined. When the 2D potential is a replica of the nonperiodic vortex structure an amplification of its interaction with the vortex structure takes place. This effect is detected only for the first matching field, becoming negligible for other matching fields. On the other hand, a periodic 2D perturbation is shown to transform the nonperiodic Bragg glass-like structure into an Abrikosov crystal with an effective Debye–Waller factor.

2D pinning potentials | vortex matter

Vortices nucleated in superconductors tend to form ordered structures. In ideally isotropic samples, free of atomic crystalline defects, the ground-state vortex structure is the Abrikosov crystal (1), a periodic elastic lattice with hexagonal symmetry. However, even high-quality single crystals have a large density of atomic defects when compared with that of vortices. The presence of atomic defects interacting with the vortex system destroys the periodicity of the Abrikosov lattice and breaks its continuous translational symmetry (2).

The response of an elastic periodic system to the presence of a dense distribution of pinning centers has been the subject of sustained theoretical and experimental interest (refs. 2 and 3 and references therein). The discovery of high-temperature superconductors and the experimental study of their vortex structures triggered a renewed interest in this problem. In recent years a new type of quasi-ordered structure, the Bragg glass, has been proposed (4) as the ground state of a vortex system interacting with a dense random distribution of atomic defects. Within this model, the long-range positional order of the Abrikosov crystal is lost but the long-range orientational correlation is preserved (4). In this hexatic vortex structure no topological defects are present at zero temperature.

In the case of high-T_c superconductors, it is widely accepted (2) that a vortex liquid phase is stable at high temperatures as a consequence of the collective vortex response to the disorder induced by point defects and thermal energy. When cooling high-quality superconducting samples in a presence of a magnetic field, field cooling, the vortex liquid state transforms into a vortex solid through a first-order phase transition (5–7). The structure of the vortex solid at low magnetic fields can be detected in real space with single-vortex sensitivity by means of the magnetic decoration technique (8). In the case of the extremely anisotropic $Bi_2Sr_2CaCu_2O_8$ system studied in this work, magnetization measurements as a function of temperature show that the irreversibility line, the temperature at which the bulk pinning sets in, $T_i(H)$, coincides with, or is very close to, the melting line (6, 7). As a consequence, despite the vortex decoration being performed at low temperatures, the observed structure corresponds to that frozen at $T_i(H)$ (9). In this way, the combination of magnetization measurements (10) and vortex magnetic decoration (9, 11) makes evident that the vortex mobility at the liquid–solid-phase transition is large enough to avoid the formation of grain boundaries.

Taking into account the structural similarities between the proposed Bragg glass and the detected high-T_c superconductors vortex structure, the low density of topological defects found in the last case could be considered as a manifestation of an out-of-equilibrium feature associated with the freezing of the structure in field cooling processes (11). This conclusion is further supported by recent experiments and numerical simulations indicating that the Bragg glass is the equilibrium vortex phase at low magnetic fields (12–14).

A magnetic decoration image of the $Bi_2Sr_2CaCu_2O_8$ vortex structure field-cooled at 36 G is shown in Fig. 1*a*. The Delaunay triangulation of this structure reveals that a low density of vortices are involved in topological defects (2% in average) (see Fig. 1*b*). Fig. 1*c* shows the positional correlation function of the structure, $G_K(r)$ (15), obtained from the measured vortex displacements with reference to the sites of a perfect hexagonal lattice. The correlation function considered in this work is an average of the positional correlation functions evaluated in the three principal directions of the vortex structure. The $G_K(r)$ shown in Fig. 1*c* was calculated in a particularly chosen region with 1,000 vortices and no dislocations. The space dependence of the positional correlation function indicates that the $Bi_2Sr_2CaCu_2O_8$ vortex structure has a positional order¶ consistent with that of the Bragg glass (4).

In previous work we demonstrated (9) that the 2D pinning potential induced by the Fe clumps produced by a first magnetic decoration of the $Bi_2Sr_2CaCu_2O_8$ vortex structure, the Bitter pinning, breaks the translational symmetry of a second vortex structure nucleated in the first matching condition. Fig. 1*d* shows the result of a second decoration of the vortex structure nucleated when field cooling the Bitter patterned sample, from room temperature down to 4.2 K, at the same magnetic field used in the first decoration. The observed perfect coincidence between both structures indicates that the second vortex structure copies the positions of the Fe clumps, including the location of the 2% of vortices associated with topological defects. This result was interpreted (9) as the consequence of an amplification of the

See accompanying Biography on page 3895.

†To whom correspondence should be sent at the present address: Département de Physique de la Matière Condensée, Université de Genève, 1211 Geneva, Switzerland. E-mail: yanina.fasano@physics.unige.ch.

§Present address: Department of Physics and Astronomy, Faculty of Sciences, Vrije Universiteit, 1081HV Amsterdam, The Netherlands.

¶The analysis of the data makes evident that the vortex system shown in Fig. 1 has long-range orientational order.

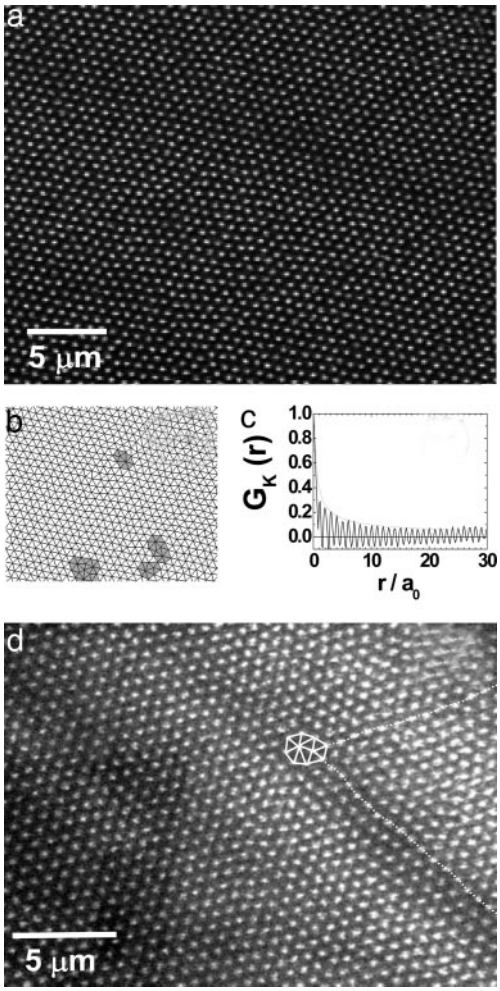

Fig. 1. $Bi_2Sr_2CaCu_2O_8$ vortex structure at low fields. (*a*) Magnetic decoration of the $Bi_2Sr_2CaCu_2O_8$ vortex structure field-cooled at 36 G. (*b*) Delaunay triangulation of the lower-right part of the structure shown in *a* where first neighbors are bonded with black lines and the non-6-fold coordinated vortices are depicted in gray. (*c*) Positional correlation function of the structure evaluated in a region with 1,000 vortices without topological defects. (*d*) Magnetic decoration of a vortex structure nucleated in the first matching condition ($B = 36$ G) with a Bitter pinning structure. It is indicated as an edge dislocation present in the Bitter pattern and reproduced by the vortex structure. The extra planes associated to it are indicated by white lines.

interaction of the vortex structure with the surface pinning potential in the case of the first matching field.

The matching between the 3D elastic system with short-range positional and long-range orientational order and the Bitter pinning is similar to the interaction of a harmonic elastic system with a commensurate rigid potential (16). On the other hand, the lack of long-range positional order of both structures makes it difficult to extend the usual concept of matching to the case of the interaction between nonperiodic elastic and rigid lattices. One possible interpretation of the Bitter pinning results is to consider that matching is a trivial consequence of the individual interaction of each Fe clump with the extremity of each vortex string. If this were the case, the pinning energy would be strong enough to compensate for the elastic energy associated with the distortions induced at the extremities of vortex strings when profiting from the pinning sites.

In this article we experimentally investigate the origin of the commensurability between rigid 2D potentials and 3D elastic structures with quasi-long-range positional order. We have been able to detect the conditions for matching between structures. In addition, we show that the vortex Bragg glass-like structure is unstable when interacting with a weak 2D periodic perturbation.

Materials and Methods

The results presented in this article were obtained by studying the interaction of 3D $Bi_2Sr_2CaCu_2O_8$ vortex structures with 2D surface pinning potentials, induced by either the Bitter pinning or periodic patterns of Fe dots. The investigated $Bi_2Sr_2CaCu_2O_8$ single crystals have a platelet shape with $\approx$1-mm^2 area, 50-μm thickness, and a critical temperature, T_c, of 86 K.

The Bitter pinning was patterned as described (9) by depositing Fe clumps through a first magnetic decoration of the vortex structure. The 2D periodic pinning potentials were engineered in the crystal surfaces by electron beam lithographed Fe dots. These had a coin shape of $\approx$60 nm in height and radii R_D varying between 100 and 200 nm. In this way, perfectly hexagonal pinning structures with typically 50×50 sites were patterned (covering an area of the order of 50×50 μm^2) (17). Regions of the crystal were left free of Fe clumps or dots (pristine regions) to comparatively study the perturbations induced by both the superficial and bulk pinning potentials.

In all of the experiments presented in this article the vortex structure was simultaneously nucleated in pristine and patterned areas by field cooling the sample with a magnetic field applied parallel to the *c* axis of the crystal. The magnitude of $B = \Phi_0/(a_0/1.075)^2$, where a_0 is the average vortex spacing, was chosen to have a commensurate density of vortices as compared with that of Fe dots or clumps, depending on the type of surface pinning potential investigated. For the particular case of the first matching field the density of vortices coincides with that of pinning centers. In the case of the Bitter pinning, this experimental condition was achieved by nucleating the vortex structure with the same magnetic field applied during the first vortex decoration; in the case of the periodic pinning patterns it was accomplished by generating the vortex structure in crystals with tens of Fe patterns with lattice parameters a_h varying in steps of parts per thousands of a_0.

Vortex positions were detected by means of the magnetic decoration technique (8) consisting of the evaporation of nanometric Fe particles that are magnetically attracted to the sites where vortices merge from the sample surface. In this way, pyramidal-shaped Fe clumps are deposited in the surface of the crystal decorating the vortex structure (18). In the experiments discussed here the vortex structure was field-cooled down to 4.2 K and decorated at this temperature. The clumps depicting vortex positions were observed by scanning electron microscopy after warming up the crystal to room temperature. In this way, the relative displacements of vortices with respect to the centers of Fe dots or clumps can be detected. The irregular shape of the Fe clumps decorating vortices allowed us to distinguish them from the circularly shaped Fe dots of the pinning structure.

Results and Discussion

To investigate whether the amplification effect induced by the Bitter pinning in the first matching field experiments (9) is a consequence of an individual vortex response, we decorated field-cooled vortex structures nucleated in the presence of commensurate Bitter patterns. In these experiments the density of vortices is 4 and 1/4 times that of pinning sites (experiments for matching fields 4 and 1/4, respectively). Fig. 2 *a* and *b* shows decoration results for the case of matching field 4, where the vortex structure has a density $B = 80$ G and the Bitter pinning was generated by decorating a $B = 20$-G vortex structure. The result obtained for a matching field of 1/4 is shown in Fig. 2*d*; in this case, the vortex structure has $B = 20$ G and the Bitter pinning was generated by decorating a $B = 80$-G vortex struc-

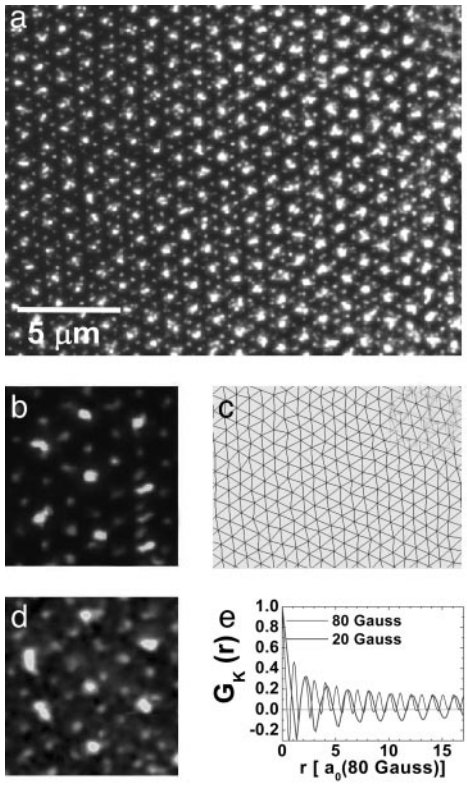

Fig. 2. Vortex structure interacting with the Bitter pinning for matching fields 4y 1/4. (*a*) Magnetic decoration of the $Bi_2Sr_2CaCu_2O_8$ vortex structure field-cooled at $B = 80$ G interacting with a Bitter pinning structure generated by a first decoration of a $B = 20$ G vortex structure (fourth matching field experiments). The pinning sites and vortices correspond to bigger and smaller Fe clumps, respectively. (*b*) Zoom-in of the pattern shown in *a*. (*c*) Delaunay triangulation of the Bitter pinning structure shown in *a* with no topological defects. (*d*) Zoom-in of a magnetic decoration of the vortex structure field-cooled at $B = 20$ G interacting with a Bitter pinning pattern generated by a first decoration of a $B = 80$-G vortex structure (1/4 matching field experiments). In this case pinning sites correspond to smaller Fe clumps, whereas the vortex positions correspond to the larger Fe clumps. (e) Positional correlation functions for the $B = 80$-G and 20-G structures.

ture. The results reveal that for matching fields 4 and 1/4 a superposition of vortex and Fe structures is not detected in extended regions of the sample. Another way to make this result evident is found in Fig. 3, which shows the Delaunay triangulation evaluated considering the positions of vortices in the first (20 G) and second (80 G) decorations. As the pinning pattern presents no topological defects in this region (see Fig. 2*c*), and as the 80-G vortex structure has a low density of them (only 1% of vortices involved), the large number of fictitious topological defects in the Delaunay triangulation shown in Fig. 3 makes evident the lack of superposition between structures in extended regions of the sample. This result is independent of whether the ratio between the densities of vortices and pinning sites is smaller or larger than one (softer and harder vortex structures, respectively). On the other hand, the results provide clear evidence of the collective nature of the interaction between elastic and rigid structures for the case of the first matching field.

The previous results indicate that the response of the Bragg glass-like 3D elastic system to the Bitter pinning is equivalent to that of a harmonic elastic system under the influence of a commensurate rigid potential only for the first matching field. They suggest that the concept of a matching condition between periodic structures could be generalized to systems with quasi-long-range positional order.

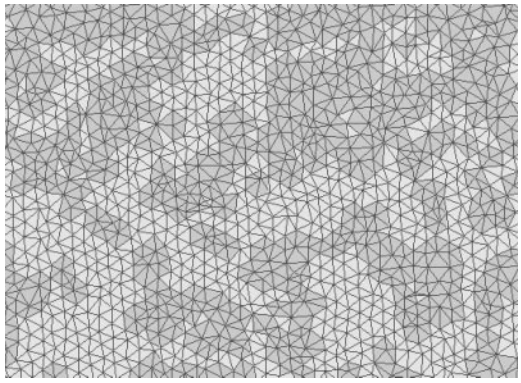

Fig. 3. Delaunay triangulation of the positions of vortices (structure nucleated at 80 G) and pinning sites (structure nucleated at 20 G) of Fig. 2*a*. The local lack of coincidence between both structures generates extra positions in the 80-G structure, leading to the fictitious topological defects observed in this joint triangulation.

In the case of an ideal Abrikosov lattice the matching condition is determined by the requirement that the ratio between the lattice parameter of the elastic system and that of the rigid potential is a rational number. This condition is univocally determined by the selection of the adequate magnetic field. However, the commensurability condition between elastic structures with quasi-long-range positional order and a rigid potential is more subtle.

It is interesting to realize that the distortions induced in the Abrikosov crystal by a dense distribution of bulk pinning centers are determined by the field-dependent elastic constants of the lattice. As a consequence, each magnetic field determines a corresponding positional correlation function $G_K(r)$, see for example Fig. 2*e*. Although the vortex structures for a given magnetic field in different experimental realizations have the same $G_K(r)$, the particular positions of vortices in the sample vary from one experiment to another. The observed perfect superposition of the distorted elastic vortex structure on top of the Fe clumps in the first matching field indicates that the Bitter pinning breaks the degeneracy of equivalent structures in different experimental realizations. Thus, the matching between structures is accomplished by involving the same deformation as that already induced in the elastic system by the presence of a dense distribution of bulk pinning centers. Obviously, this is not the case for matching fields different from one. In this case, the experimental results shown in Fig. 2 demonstrate that the pinning force associated with the Bitter pinning is not strong enough to induce the necessary extra deformation of the 3D vortex structure required to match the rigid potential.

The previous results show that the Bitter pinning breaks the degeneracy of equivalent structures in the case of the first matching field. Then, it is interesting to ask whether in this case an equally weak but periodic hexagonal structure of Fe dots could destabilize the Bragg glass.

The stability of the quasi-long-range positionally ordered vortex structure under the presence of a 2D periodic hexagonal perturbation was studied in samples with periodic patterns of Fe dots generated as described in *Materials and Methods*. It is important to remark that the field-cooled vortex structures in the range of fields we considered have $\approx 2\%$ of vortices involved in dislocations. Thus, the recovery of a periodic hexagonal vortex structure would imply not only the suppression of the accumulative distortions induced by the bulk pinning but also the generation of the elastic and plastic distortions required to remove the topological defects.

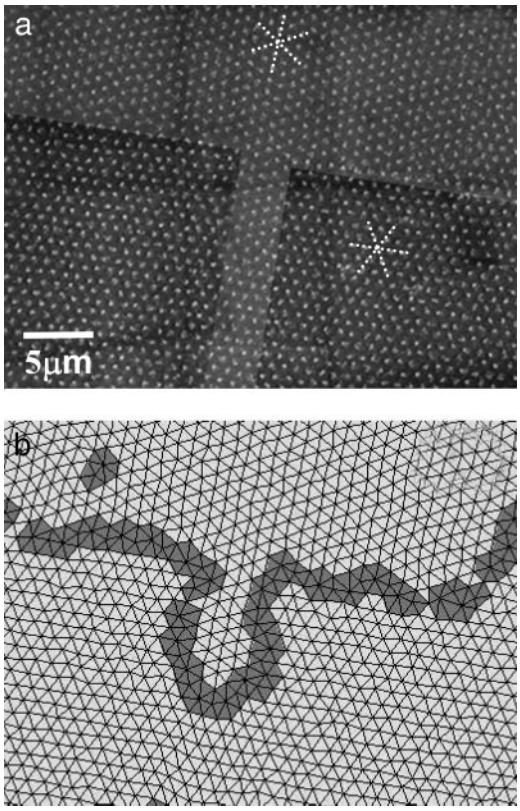

Fig. 4. Vortex structure interacting with a periodic hexagonal pinning potential. (*a*) Magnetic decoration of the $Bi_2Sr_2CaCu_2O_8$ vortex structure field-cooled at 30.9 G nucleated in pristine regions and in the presence of a hexagonal superficial pinning potential (dark areas) for the first matching field. The compact planes of the lattice in both regions are depicted with white-dotted lines. In the patterned regions they coincide with the principal directions of the hexagonal pinning structure. (*b*) Delaunay triangulation of the vortex structure where non-6-fold coordinated vortices are depicted in gray.

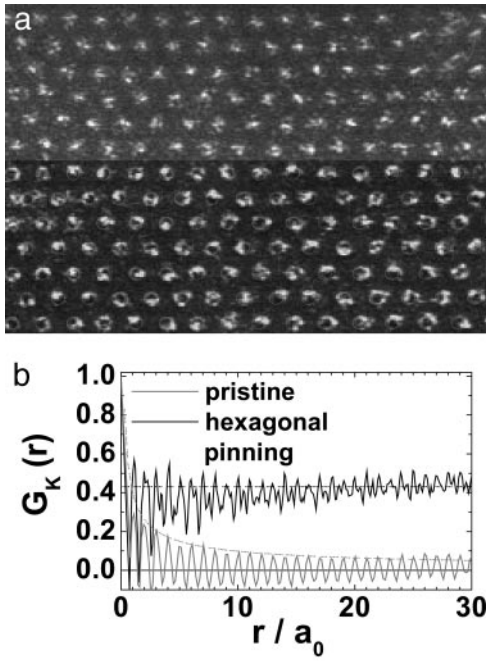

Fig. 5. Effect of the hexagonal pinning acting on the vortex structure. (*a*) Magnetic decoration of the $Bi_2Sr_2CaCu_2O_8$ vortex structure field-cooled at 30.9 G nucleated in the neighborhood of a hexagonal superficial pinning potential (darker region). The positions of the electron-beam lithographed Fe dots are superimposed with circles. (*b*) Positional correlation functions of the vortex lattice nucleated in pristine and patterned regions. In the first case, the fitted algebraic decay (dotted line) indicates that the order of the vortex structure is compatible with the quasi-long-range positional order characteristic of the Bragg glass. In the second case, the oscilation around the value of 0.43 at long distances reveals that the structure has long-range positional order.

Fig. 4 shows the magnetic decoration of a field-cooled vortex structure nucleated in the neighborhood of a perfectly hexagonal pinning potential with $a_h = 0.88$ μm and $R_D = 130$ nm in the case of the first matching field (30.9 G). The decoration image of Fig. 4 is an example of a vortex structure nucleated in pristine regions with compact planes misaligned with respect to those of the pinning lattice. As shown in Fig. 4*b*, this misalignment induces grain boundaries at the edge of patterned regions. A zoomed image, as shown in Fig. 5*a*, shows the distinction of the irregular Fe clumps of the vortex decoration from the circular Fe dots, revealing that vortices are localized within the dots in one-to-one correspondence.

One of the conditions necessary to recover the periodic structure is accomplished: no dislocations in the vortex structure were detected in patterned regions, as demonstrated by the Delaunay triangulation shown in Fig. 4*b*. This one-to-one correspondence between vortices and Fe dots makes evident the relevance of the weak periodic potential for transforming the structure with quasi-long-range positional order into a hexagonal lattice. This result implies that the long-range positional order of the structure is established by a collective response of the vortex structure nucleated in the presence of periodic pinning. However, the detected random displacements of vortices with respect to the centers of Fe dots within the limit of R_D indicates the effect of the bulk pinning potential.

The characterization of the positional order of the structure nucleated in patterned regions is done by analyzing its positional correlation function. Fig. 5*b* shows the comparison of $G_K(r)$ for the vortex structures nucleated in pristine (same curve as in Fig. 1*c*) and hexagonal patterned areas. In the first case $G_K(r)$ was calculated in a region free of dislocations to avoid the local suppression of the positional order induced by them. It can be seen that $G_K(r)$ in the pristine area decays at long distances with a functionality consistent with the quasi-long-range positional order characteristic of the Bragg glass. In contrast, the $G_K(r)$ of the vortex lattice nucleated in the hexagonal-patterned areas oscillates at long distances around a finite value, smaller than the value of 1 corresponding to a perfect geometrical lattice. This result shows that the hexagonal superficial Fe structure induces long-range positional order on the vortex structure. As mentioned, the bulk pinning induces random nonaccumulative vortex displacements around the geometrical sites of a perfect lattice. This finding is in contrast with the accumulative vortex displacements detected in the vortex structure nucleated in pristine regions.

The vortex displacements around the sites of a perfect hexagonal lattice are approximated with a Gaussian distribution with mean value δ. Within this approximation, the saturation at long distances of $G_K(r) = \exp(-(K.\delta)^2/2) \approx 1 - 1/2(K.\delta)^2 \approx 0.43$ allows us to estimate an average displacement $\delta \approx 0.15$ μm, of the order of the dots radius, $R_D = 0.13$ μm. This result supports the idea that the displacements induced by bulk pinning are confined to amplitudes within the range of the pinning force induced by the Fe dots.

The one-to-one correspondence between Fe dots and vortices, the suppression of the dilute density of dislocations, and the random displacements of vortices around the geometrical sites of

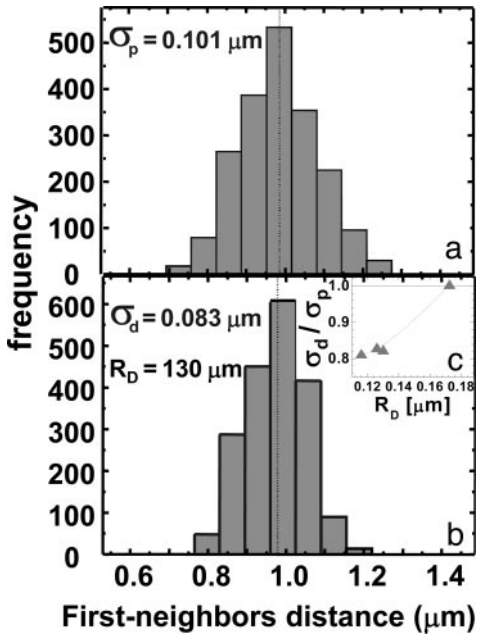

Fig. 6. Vortex localization induced by the dots of the hexagonal pinning. (*a* and *b*) Distribution of first-neighbors distance for the vortex structure nucleated in pristine (*a*) and patterned (*b*) regions with standard deviations σ_P and σ_D, respectively. (*c*) Evolution of the normalized standard deviation σ_D/σ_P as a function of the radius of dots, R_D. The line between points is a guide for the eye.

the periodic pinning strongly suggest that the Bragg glass-like structure is unstable in the presence of a weak perfectly hexagonal perturbation. Moreover, the standard deviation of the first-neighbors distance distribution, σ, is 18% smaller for the vortex structure nucleated in patterned regions than for that nucleated in pristine regions (see Fig. 6 *a* and *b*).

This behavior confirms that the displacements of vortices with respect to a perfect hexagonal lattice are decreased as compared with that of the Bragg glass-like structure. The random noncorrelated displacements of vortices around the sites of a perfect lattice are easily interpreted as caused by a Debye–Waller factor with an effective temperature that simulates the effect of the randomly distributed bulk pinning. The localization of vortices within the diameter of the Fe dots is consistent with the proposed collective response of the vortex structure. Within this picture, the Debye–Waller temperature associated with bulk disorder should decrease by decreasing the Fe dots radii. This effect is evident from the R_D evolution of the standard deviation of the first-neighbors distance distribution (see Fig. 6*c*).

Conclusions

We have engineered periodic and nonperiodic surface pinning potentials interacting with 3D superconducting vortex structures. In the experiments, the length of vortices was orders of magnitude larger than the height of pinning centers. In this way, a weak pinning potential was introduced at the extremities of a collection of interacting strings nucleated in the presence of the quenched atomic disorder of the superconducting crystal. The distortion of the Abrikosov crystal associated with bulk pinning gives rise to a structure characterized by quasi-long-range positional and long-range orientational correlation, consistent with the proposed Bragg glass. As would be expected, the superficial potential has no detectable effect on the vortex structure except at rather stringent conditions.

When the surface pinning pattern has the same positional correlation function as the vortex system, it is detected that both structures match. This finding implies that the Bitter pinning breaks the translational symmetry of the system under different experimental realizations. Perfect localization of vortices within the size of pinning sites is detected. On the other hand, when the superficial pinning structure is periodic the amplification effect is strong enough to transform the vortex structure with quasi-long-range positional order into a localized hexagonal lattice with an effective Debye–Waller factor.

The observation of vortex structures in extended regions of the surface of a sample has allowed the study and detection of two types of vortex localizations induced by extremely weak perturbations acting on elastic nonperiodic systems. It is important to take into account that our conclusions and suggestions are based on real-space observations of structures that have been frozen after a first-order phase transition at high temperatures. Then, it is reasonable to consider whether the amplification effect induced by matching nonperiodic systems could have an effect on the temperature where the space-localized vortices (solid) make the transition into a delocalized system of interacting strings (liquid). This possible scenario stimulates theoretical and experimental studies focalized on the detection of a possible shifting of the melting temperature and on the topological characteristics of the structural transformation produced at the liquid–solid-phase transition.

We thank G. Nieva (Instituto Balseiro and Centro Atómico Bariloche, Comisión Nacional de Energia Atómica) for providing the samples. This work was supported by Agencia Nacional de Promoción Científica y Tecnológica Grant PICT99-5117 and the Fundación Antorchas.

1. Abrikosov, A. A. (1957) *Soviet Physics JETP* **5,** 1174–1182.
2. Blatter, G., Feigel'man, M. V., Geshkenbein, V. B., Larkin, A. I. & Vinokur, V. M. (1994) *Rev. Mod. Phys.* **66,** 1125–1388.
3. Giamarchi, T. & Bhattacharya, S. (2002) in *High Magnetic Fields Applications in Condensed Matter Physics and Spectroscopy*, ed. Berthier, C. (Springer, Berlin), pp. 314–362.
4. Giamarchi, T. & Le Doussal, P. (1994) *Phys. Rev. Lett.* **72**, 1530–1533.
5. Safar, H., Gammel, P. L., Huse, D. H., Bishop, D. J., Rice, J. P. & Ginsberg, D. M. (1992) *Phys. Rev. Lett.* **69,** 824–827.
6. Pastoriza, H., Goffman, M. F., Arribere, A. & de la Cruz, F. (1994) *Phys. Rev. Lett.* **72,** 2951–2954.
7. Zeldov, E., Majer, D., Konczykowski, M., Geshkenbein, V. B., Vinokur, V. M. & Shtrikman, H. (1995) *Nature* **375,** 373–376.
8. Träuble, H. & Essmann, U. (1967) *Phys. Lett. A* **24,** 526–527.
9. Fasano, Y., Menghini, M., Nieva, G. & de la Cruz, F. (2000) *Phys. Rev. B* **62,** 15183–15189.
10. Correa, V. F., Nieva, G. & de la Cruz, F. (2001) *Phys. Rev. Lett.* **87,** 057003–057006.
11. Kim, P., Yao, Z., Bolle, C. A. & Lieber, C. (1999) *Phys. Rev. B* **60,** R12589–R12592.
12. Klein, T., Joumard, I., Blanchard, S., Marcus, J., Cubbit, R., Giamarchi, T. & Le Doussal, P. (2001) *Nature* **413,** 404–406.
13. Gingras, M. J. P. & Huse, D. A. (1996) *Phys. Rev. B* **53,** 15193–15200.
14. van Otterlo, A., Scalettar, R. T. & Zimányi, G. T. (1998) *Phys. Rev. Lett.* **81,** 1497–1500.
15. Halperin, B. I. & Nelson, D. R. (1978) *Phys. Rev. Lett.* **41,** 121–124.
16. Chaikin, P. M. & Lubensky, T. C. (1995) *Principles of Condensed Matter Physics* (Cambridge Univ. Press, Cambridge, U.K.).
17. Fasano, Y., de Seta, M., Menghini, M., Pastoriza, H. & de la Cruz, F. (2003) *Sol. State Commun.* **128,** 51–56.
18. de la Cruz, F., Menghini, M. & Fasano, Y. (2000) *Condens. Matter Theor.* **16,** 275–284.